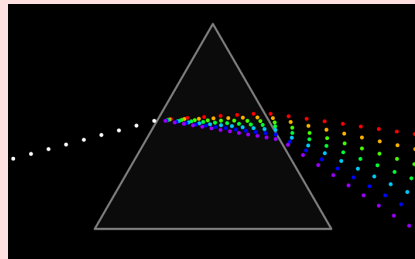


Presision Physics for Fundamental Physics

V.I. Korobov

Joint Institute for Nuclear Research
141980, Dubna, Russia



Dubna, June, 2025

Introduction

What is precision physics?

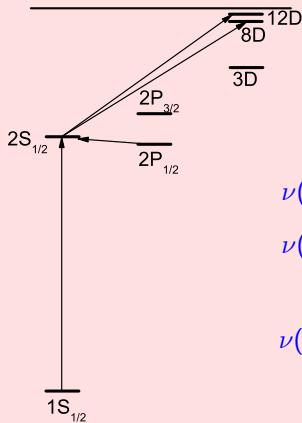
- ➊ What can we measure with very high precision — frequency!
Second is currently defined as the duration of 9 192 631 770 periods of the radiation corresponding to the transition between *the two hyperfine levels of the ground state of the caesium 133 atom.*
- ➋ Hydrogen atom and positronium
- ➌ Precision Spectroscopy of the Hydrogen molecular ions
- ➍ Physics of exotic atoms

Introduction

What can we get studying precision physics?

- ① Tight constrains on new forces
- ② Fundamental physical constants
- ③ Variation of fundamental constants with time.
- ④ Tests of the CPT invariance
- ⑤ Properties of exotic particles like muon, pion, kaon, etc.

Rydberg constant from hydrogen atom



$$\nu(2S_{1/2} - 12D_{5/2}) = 799\,191\,727.403\,7(47) \text{ MHz}$$

$$\nu(1S_{1/2} - 2S_{1/2}) = 2\,466\,061\,413.187\,018(11) \text{ MHz}$$

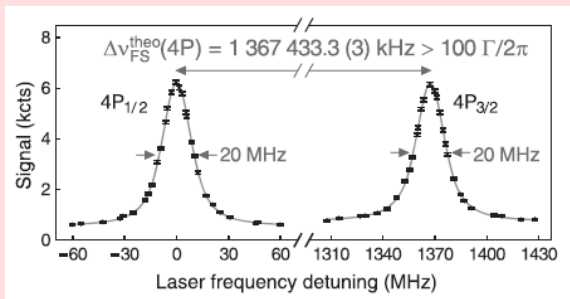
$$\nu(\text{HFS}) = 1\,420.405\,751\,768(2) \text{ MHz}$$

$$R_\infty c = 3.289\,841\,960\,2500(36) \times 10^{15} \text{ Hz}$$

Rydberg constant. MPQ experiment, Garching.

$1S-4P$ transition.

A. Bayer, et al. Science 358, 79 (2017).



conservation. (B) Typical experimental fluorescence signal from a single line scan over the $2S-4P_{1/2}$ (left) and $2S-4P_{3/2}$ (right) resonance (black diamonds). The observed line width (full width at half maximum) of $\sim 2\pi \times 20 \text{ MHz}$ is larger than the natural line width $\Gamma = 2\pi \times 12.9 \text{ MHz}$ because of Doppler and power broadening. The accuracy of our measurement corresponds to almost 1 part in 10,000 of the observed line width. The constant background counts are caused by the decay of $2S$ atoms inside the detector (17). kcts, kilocounts.

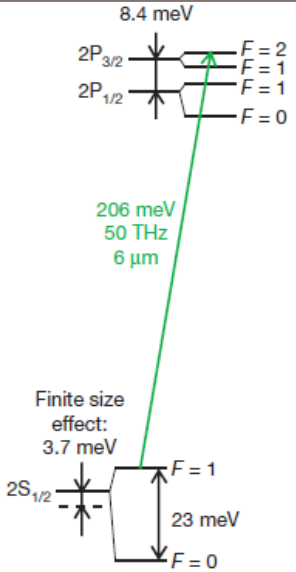
Proton charge radius puzzle. First experiment.

Randolf Pohl, et al. (CREMA Collab.)

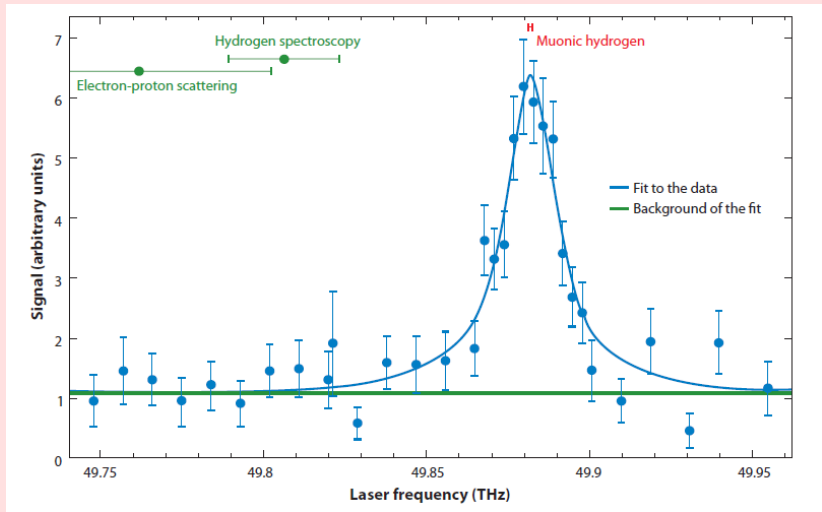
The Size of the proton.

Nature 466, 213 (2010).

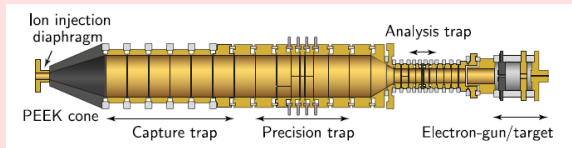
The charge radius of the proton from muonic hydrogen spectroscopy should be $r_p = 0.84184(67) \text{ fm}$ while the CODATA06 recommended value is 5σ off $r_p = 0.8768(69) \text{ fm}$



Proton charge radius puzzle



Penning trap experiments

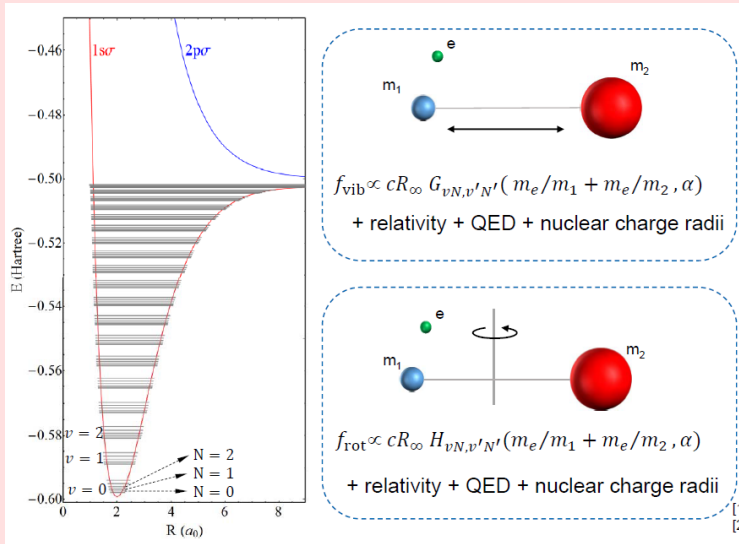


The ALPHATRAP tower. The precision trap is used for high-precision spectroscopy and the analysis trap is used for the state determination.

Precision measurements:

- electron g -factor measurements;
- proton and other nuclei magnetic moments;
- Mass ratios;
- Vibrational and HFS transitions in the molecular ions.

Molecular ion spectroscopy



Molecular ion spectroscopy in the RF trap

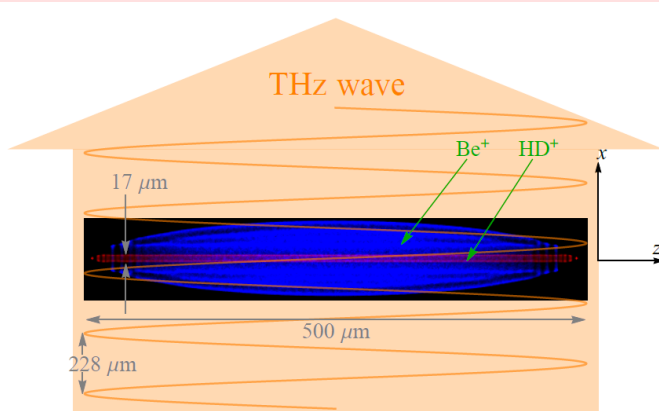


FIG. 1. Principle of the Lamb-Dicke rotational spectroscopy of sympathetically cooled molecular ions. The ion cluster is prolate, and the sympathetically cooled ions exhibit a relatively small motional range in the directions x , y perpendicular to the trap axis z . The spectroscopy radiation propagates perpendicular to z . The ion cluster image is a time average of ion trajectories

Precision physics: Theory

Nonrelativistic QED (NRQED)

Three-body problem: Helium atom

PHYSICAL REVIEW A 98, 012510 (2018)

Nonrelativistic energy levels of helium atoms

D. T. Aznabaev,^{1,2,3} A. K. Bekbaev,^{1,4} and Vladimir I. Korobov^{1,5}

TABLE II. Nonrelativistic energies of the S , P , D , and F states of a helium atom. N is the number of basis functions. The two lines represent two consecutive calculations with the largest basis sets to show convergent digits. The third line presents calculations by Drake and Yan [23].

State	N	E_{nr}	State	N	E_{nr}
1^1S	18000	-2.90372 43770 34119 59831 11592 45194 40432	4^1S	14000	-2.03358 67170 30725 44743 92926 44363 64
1^1S	22000	-2.90372 43770 34119 59831 11592 45194 40443	4^1S	18000	-2.03358 67170 30725 44743 92926 44363 87
2^1S	18000	-2.14597 40460 54417 41580 50289 75461 918	4^3S	14000	-2.03651 20830 98236 29958 03780 71617 853
2^1S	22000	-2.14597 40460 54417 41580 50289 75461 921	4^3S	16000	-2.03651 20830 98236 29958 03780 71617 874
[23]		-2.14597 40460 5443(5)			
2^3S	14000	-2.17522 93782 36791 30573 89782 78206 81124	4^1P	18000	-2.03106 96504 50240 71475 89314 36090 3
2^3S	16000	-2.17522 93782 36791 30573 89782 78206 81125	4^1P	22000	-2.03106 96504 50240 71475 89314 36094 1
[23]		-2.17522 93782 367912(1)		[23]	-2.03106 96504 5024(3)
2^1P	18000	-2.12384 30864 98101 35924 73331 42354	4^3P	18000	-2.03232 43542 96630 33195 38824 67087
2^1P	22000	-2.12384 30864 98101 35924 73331 42374	4^3P	22000	-2.03232 43542 96630 33195 38824 67103
[23]		-2.12384 30864 98092(8)		[23]	-2.03232 43542 9662(2)
2^3P	16000	-2.13316 41907 79283 20514 69927 63793	4^1D	22000	-2.03127 98461 78684 99621 39438 073
2^3P	18000	-2.13316 41907 79283 20514 69927 63806	4^1D	26000	-2.03127 98461 78684 99621 39438 143
[23]		-2.13316 41907 7927(1)		[23]	-2.03127 98461 78687(7)
3^1S	18000	-2.06127 19897 40908 65074 03499 37089 2816	4^3D	18000	-2.03128 88475 01795 53802 34920 591
3^1S	22000	-2.06127 19897 40908 65074 03499 37089 2824	4^3D	22000	-2.03128 88475 01795 53802 34920 630
[23]		-2.03128 88475 01795(3)			
3^3S	14000	-2.06868 90674 72457 19199 65329 11291 75048	4^1F	18000	-2.03125 51443 81748 60863 20824 071
3^3S	16000	-2.06868 90674 72457 19199 65329 11291 75049	4^1F	22000	-2.03125 51443 81748 60863 20824 079
[23]		-2.03125 51443 81749(1)			



Concept of NRQED

QED

$$\mathcal{L}_{\text{QED}} = \bar{\psi} [(i\partial - e A) \gamma - m] \psi - \frac{1}{4} F_{\mu\nu} F^{\mu\nu},$$



Nonrelativistic QED

$$\mathcal{L}_{\text{NRQED}}$$



Effective Hamiltonian

$$H_{\text{eff}} = \sum_i \frac{\mathbf{P}_i^2}{2m_i} + e^2 \sum_{j>i} \frac{Z_i Z_j}{r_{ij}} + \text{higher order corrections}$$

(Here $\mathbf{P}_i = \mathbf{p}_i + e\mathbf{A}$)

Nonrelativistic QED Lagrangian

The Lagrangian for NRQED is built out nonrelativistic (two-component) Pauli spinor fields ψ for each of the electron, positron, muon, proton, etc. Photons are treated in the same fashion as in QED.

$$\begin{aligned}
 L_{\text{eff}} = & -\frac{1}{2}(E^2 - B^2) + \psi_e^* \left(i\partial_t - e\varphi + \frac{\mathbf{D}^2}{2m} + \frac{\mathbf{D}^4}{8m^3} + \dots \right) \psi_e \\
 & + \psi_e^* \left(c_F \frac{e}{2m} \boldsymbol{\sigma} \mathbf{B} + c_D \frac{e}{8m^2} [\mathbf{D}\mathbf{E}] + c_S \frac{e}{8m^2} \{ \boldsymbol{\sigma} \cdot [i\mathbf{D} \times \mathbf{E}] \} \right) \psi_e \\
 & + \text{higher order terms} + \text{muon, proton, etc.} \\
 & - \frac{d_1}{m_e m_\ell} (\psi_e^* \boldsymbol{\sigma}_e \psi_e) (\psi_\ell^* \boldsymbol{\sigma}_\ell \psi_\ell) + \frac{d_2}{m_e m_\ell} (\psi_e^* \psi_e) (\psi_\ell^* \psi_\ell) + \dots
 \end{aligned}$$

where $\mathbf{D} = \nabla - ie\mathbf{A}$.

$$c_D = 1 + 2\kappa + \frac{\alpha}{\pi} \frac{8}{3} \left[\ln \left(\frac{m}{2\Lambda} \right) + \frac{5}{6} - \frac{3}{8} \right],$$

$$c_S = 1 + 2\kappa,$$

$$c_F = 1 + \kappa,$$

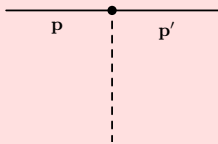
$$d_1 = (Z\alpha)^2 \frac{2}{m_e^2 - m_\ell^2} \ln \left(\frac{m_e}{m_\ell} \right),$$

$$d_2 = (Z\alpha)^2 \left\{ \frac{7}{3} - 2 \ln \left(\frac{m}{2\Lambda} \right) + \frac{2}{m_e^2 - m_\ell^2} \left[m_e^2 \ln \left(\frac{m_\ell}{\mu} \right) - m_\ell^2 \ln \left(\frac{m_e}{\mu} \right) \right] \right\}.$$

Examples of basic interactions in NRQED. Vertices.

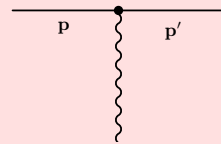
Coulomb

$$e$$



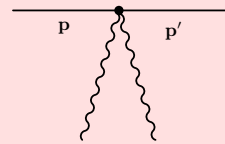
"dipole"

$$-e \left[\frac{p' + p}{2m} \right]$$



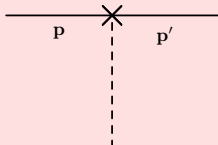
\mathbf{A}^2

$$e^2 \left[\frac{\delta^{ij}}{2m} \right]$$



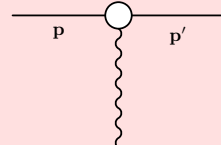
Darwin's

$$-e \left[\frac{1}{8m^2} \right] \mathbf{q}^2$$



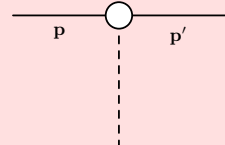
Fermi's

$$e \left[\frac{i}{2m} \right] (\mathbf{q} \times \boldsymbol{\sigma})$$



spin-orbit

$$e \left[\frac{i}{4m^2} \right] (\mathbf{p}' \times \mathbf{p}) \cdot \boldsymbol{\sigma}$$



Here $\mathbf{q} = \mathbf{p}' - \mathbf{p}$ is a transferred impulse of the particle.

NRQED propagators

A natural choice of a gauge for the electromagnetic field is the Coulomb gauge ($\mathbf{kA} = 0$)

$$\begin{cases} G^{00} = \frac{1}{\mathbf{k}^2}, & \text{— the Coulomb photon propagator,} \\ G^{ij} = \frac{\delta_{ij} - k_i k_j / \mathbf{k}^2}{\mathbf{k}^2 + i\varepsilon}, & \text{— the transverse photon propagator,} \\ G^{0i} = G^{i0} = 0, \quad i, j = 1, 2, 3. & \end{cases}$$

For exchange photons $k_0 \approx m\alpha^2$ and

$$G^{ij} \approx -\frac{1}{\mathbf{k}^2} \left[\delta_{ij} - \frac{k_i k_j}{\mathbf{k}^2} \right].$$

Propagators for massive particles

$$\frac{1}{E - \mathbf{p}^2/(2m) + i\varepsilon}.$$

Hydrogen: Theory

$$E_{\text{nr}} = -\frac{(Z\alpha)^2}{2n^2}$$

1. One-loop self-energy:

The one-loop self-energy contribution to a binding energy of electron for the hydrogen-like ion can be expressed

$$\begin{aligned}\Delta E_{\text{1loop-se}} = & \frac{\alpha (Z\alpha)^4}{\pi n^3} \left\{ \left[A_{41}(n) \ln [(Z\alpha)^{-2}] + A_{40}(n) \right] + (Z\alpha) A_{50}(n) \right. \\ & + (Z\alpha)^2 \left[A_{62}(n) \ln^2 [(Z\alpha)^{-2}] + A_{61}(n) \ln [(Z\alpha)^{-2}] + A_{60}(n) \right] \\ & \left. + (Z\alpha)^3 \left[A_{71}(n) \ln [(Z\alpha)^{-2}] + A_{70} \right] + \dots \right\}\end{aligned}$$

Hydrogen: Theory

For the hydrogen atom in S -state the coefficients are

$$\left\{ \begin{array}{l} A_{41}(nS) = \frac{4}{3} \\ A_{40}(nS) = \left[\frac{10}{9} - \frac{4}{3} \ln k_0(nS) \right] \\ A_{50}(nS) = 4\pi \left[\frac{139}{128} - \frac{1}{2} \ln 2 \right] \\ A_{62}(nS) = [-1], \\ A_{61}(nS) = 4 \left[\frac{4}{3} \ln 2 + \ln \frac{2}{n} + \psi(n+1) - \psi(1) - \frac{601}{720} - \frac{77}{180n^2} \right], \\ A_{60}(1S) = -30.92414946\dots \\ A_{71}(nS) = \pi \left[\frac{139}{64} - \ln 2 \right] \end{array} \right.$$

Hydrogen: Theory

Other contributions:

- One-loop vacuum polarization
- The Wichman-Kroll contribution
- Two-loop and three-loop contributions
- Finite nuclear size and polarizability

The total theoretical relative uncertainty for the energy of the $1S$ state is:
 $u_r(\text{theor}) \approx 1 \cdot 10^{-12}$.

Hydrogen molecular ion H_2^+

Contributions to the *ab initio* spin-averaged transition frequency:
 $(v = 1, N = 0) \rightarrow (v' = 3, N' = 2)$

Relative order	Contribution (kHz)	Origin
α^0	124 485 554 550.93	Nonrelativistic 3-body Schrödinger equation
α^2	2 002 698.73	Relativistic corrections in Breit–Pauli approximation; finite nuclear radii
α^3	−521 345.53	Leading-order one-loop radiative corrections
α^4	−3 689.05	One- and two-loop radiative corrections relativistic corrections
α^5	310.24	Up to three-loop radiative and WK corrections
α^6	−1.07	One- and two-loop radiative diagrams; WK
other	0.54	Muon and hadron vacuum polarization
total	124 487 032 524.80	Total transition energy

Relative theoretical uncertainty: $u_r \approx 7.5 \times 10^{-12}$

HD⁺. Theory and experiment

Theoretical and experimental spin-averaged transition frequencies (in kHz). CODATA18 values of fundamental constants were used in the calculations.

$(L, \nu) \rightarrow (L', \nu')$	theory	experiment
$(0, 0) \rightarrow (1, 0)$	1 314 925 752.932(19)	1 314 925 752.910(17)
$(0, 0) \rightarrow (1, 1)$	58 605 052 163.9(0.5)	58 605 052 164.24(86)
$(3, 0) \rightarrow (3, 9)$	415 264 925 502.8(3.3)	415 264 925 501.8(1.3)

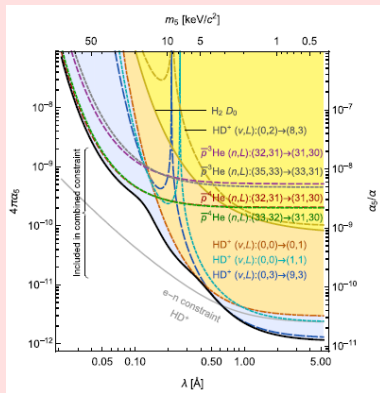
Applications for fundamental physics

New forces

Yukawa-type interaction:

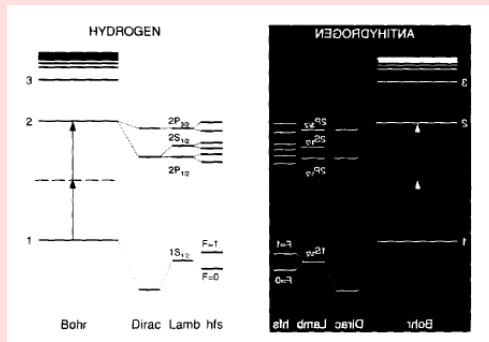
$$V_{\alpha_5,\lambda}(r) = \hbar c \alpha_5 A_1 A_2 \frac{e^{-r/\lambda}}{r},$$

where A_1 and A_2 are nucleon numbers as charges of the hypothetical interaction.



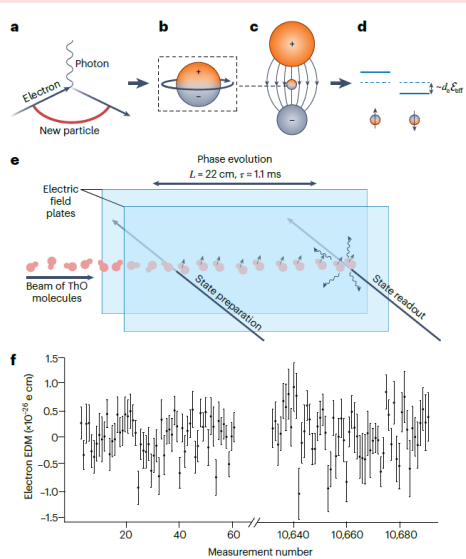
CPT tests

- Hydrogen — Antihydrogen



- Antihydrogen ion in the Penning trap

CP-violation. EDM. ACME experiment



electron EDM bounds:
 $|d_e| < 1.1 \times 10^{-29} \text{ e cm}$

mass constrain:
 $\Lambda > 30 \text{ Tev}$

Physics of exotic atoms

Antiprotonic Helium

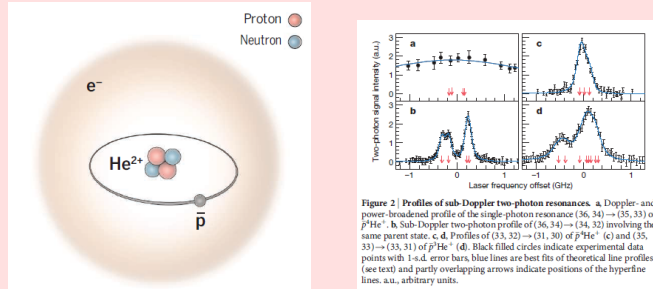


Figure 2 | Profiles of sub-Doppler two-photon resonances. a, Doppler- and power-broadened profile of the single-photon resonance $(36, 34) \rightarrow (35, 33)$ of $\bar{p}^4\text{He}^+$. b, Sub-Doppler two-photon profile of $(36, 34) \rightarrow (34, 32)$ involving the same parent state. c, d, Profiles of $(33, 32) \rightarrow (31, 30)$ of $\bar{p}^4\text{He}^+$ (c) and $(35, 33) \rightarrow (33, 31)$ of $\bar{p}^3\text{He}^+$ (d). Black filled circles indicate experimental data points with 1-s.d. error bars, blue lines are best fits of theoretical line profiles (see text) and partly overlapping arrows indicate positions of the hyperfine lines. a.u., arbitrary units.

[M. Hori et al. *Nature* **475**, 484 (2011)]

Isotope	Transition $(n, l) \rightarrow (n - 2, l - 2)$	Transition frequency (MHz)	
		Experiment	Theory
$\bar{p}^4\text{He}^+$	$(36, 34) \rightarrow (34, 32)$	1,522,107,062(4)(3)(2)	1,522,107,058.9(2.1)(0.3)
$\bar{p}^3\text{He}^+$	$(33, 32) \rightarrow (31, 30)$	2,145,054,858(5)(5)(2)	2,145,054,857.9(1.6)(0.3)
	$(35, 33) \rightarrow (33, 31)$	1,553,643,100(7)(7)(3)	1,553,643,100.7(2.2)(0.2)

Experimental values show respective total, statistical and systematic 1-s.d. errors in parentheses; theoretical values (ref. 3 and V. I. Korobov, personal communication) show respective uncertainties from uncalculated QED terms and numerical errors in parentheses.

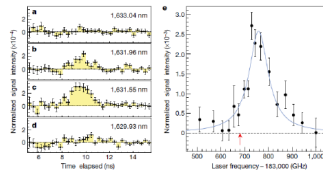
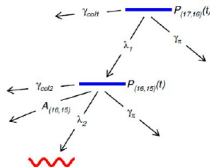
$$m_{\bar{p}}/m_e = 1836.152\,6734(15) [8 \times 10^{-10}]$$

Precision Spectroscopy of the Pionic Helium-4

Zhi-Da Bai, V.I. Korobov et al., Phys. Rev. Lett. **128**, 183001 (2022)

The theoretical transition frequency of $(n, l) = (17, 16) \rightarrow (16, 15)$ in pionic helium-4 may be calculated to an accuracy of 4 ppb, that includes relativistic and quantum electrodynamic corrections up to $O(R_\infty a^5)$. Once measurements reach the ppb level, then the accuracy of determining the **pionic mass** can achieve a relative precision of 10^{-8} .

Outcome: Such a high precision value of m_π can impose direct experimental constraints on the mass of the antineutrino of muon flavor.



Laser resonance signals of the transition

$(n, l) = (17, 16) \rightarrow (17, 15)$ in metastable $\pi^4\text{He}^*$ atoms.
M.Hori et al. Nature **581**, 37 (2020)

Precision Spectroscopy of HD⁺

HD⁺. Theory and experiment

Theoretical and experimental spin-averaged transition frequencies (in kHz). CODATA18 values of fundamental constants were used in the calculations.

$(L, \nu) \rightarrow (L', \nu')$	theory	experiment
$(0, 0) \rightarrow (1, 0)$	1 314 925 752.932(19)	1 314 925 752.910(17)
$(0, 0) \rightarrow (1, 1)$	58 605 052 163.9(0.5)	58 605 052 164.24(86)
$(3, 0) \rightarrow (3, 9)$	415 264 925 502.8(3.3)	415 264 925 501.8(1.3)

Results

Reduced mass $\mu = \frac{m_p m_d}{(m_p + m_d)m_e}$ inferred from the HD⁺ ion spectroscopy

	μ
CODATA18	1223.899 228 722(51)
$(0, 0) \rightarrow (0, 1)$	1223.899 228 743(16) _{exp} (17) _{th}
$(0, 0) \rightarrow (1, 1)$	1223.899 228 707(17) _{exp} (17) _{th}
$(3, 0) \rightarrow (3, 9)$	1223.899 228 730(04) _{exp} (17) _{th}
1223.899 228 730(04) _{exp} (17) _{th}	

Relative uncertainty: $u_r(\mu) = 1.4 \times 10^{-11}$.

Results

Reduced mass $\mu = \frac{m_p m_d}{(m_p + m_d)m_e}$ inferred from the HD⁺ ion spectroscopy

	μ
CODATA18	1223.899 228 722(51)
$(0, 0) \rightarrow (0, 1)$	1223.899 228 743(16) _{exp} (17) _{th}
$(0, 0) \rightarrow (1, 1)$	1223.899 228 707(17) _{exp} (17) _{th}
$(3, 0) \rightarrow (3, 9)$	1223.899 228 730(04) _{exp} (17) _{th}
1223.899 228 730(04)_{exp}(17)_{th}	

Relative uncertainty: $u_r(\mu) = 1.4 \times 10^{-11}$.

Mass ratios from spectroscopy and Myers' experiment:

$$m_p/m_e = 1836.152673476(44), \quad m_d/m_e = 3670.482967763(88),$$

and the new CODATA22 value is $m_p/m_e = 1836.152673426(32)$.

CODATA18 vs CODATA22

quantity	symbol	value	uncertainty
proton rms charge radius	r_p	$0.8414(19) \times 10^{-15}$ m	2.2×10^{-3}
		$0.84075(64) \times 10^{-15}$ m	7.6×10^{-4}
Rydberg constant	$R_\infty c$	$3\ 289\ 841\ 960.2500(64)$ MHz ⁻¹	1.9×10^{-12}
		$3\ 289\ 841\ 960.2500(36)$ MHz ⁻¹	1.1×10^{-12}
proton-electron mass ratio	$\mu = m_p/m_e$	$1836.152\ 673\ 43(11)$	6.0×10^{-11}
		$1836.152\ 673\ 426(32)$	1.7×10^{-11}

Thank you for your attention!